IEEE Access
Multidisciplinary | Rapid Review | Open Access Journal

Received December 10, 2019, accepted January 6, 2020, date of publication January 10, 2020, date of current version January 22, 2020.

Digital Object Identifier 10.1109/ACCESS.2020.2965773

Isolation and Protection of the Motor-Generator Pair System for Fault Ride-Through of Renewable Energy Generation Systems

YUJUN GU, (Student Member, IEEE), YONGZHANG HUANG, (Member, IEEE), QIANYU WU, (Student Member, IEEE), CHENYANG LI, (Student Member, IEEE), HAISEN ZHAO, (Member, IEEE), AND YANG ZHAN, (Member, IEEE)

State Key Laboratory of Alternate Electrical Power System with Renewable Energy Sources, North China Electric Power University, Beijing 102206, China

Corresponding author: Yujun Gu (guyujun1104@126.com)

This work was supported in part by the Science and Technology Project of State Grid under Grant XT71-18-041, and in part by the Cooperative Training Project of North China Electric Power University Scholarship Fund.

ABSTRACT Renewable energy units are required to have reliable fault ride-through capability to prevent large-scale disconnection of renewable energy plants due to grid faults. Since synchronous generators have better voltage and current resistance capabilities, one of the advantages of renewable energy connected to the grid through the motor-generator Pair (MGP) system is the isolation of grid faults, which is totally different from existing fault ride-through methods. First, the structure and mathematical model of the MGP system are introduced in this paper. Then, a novel control method for the MGP system based on DC link voltage feedback is given, which is very important for fault ride-through in the control power balance on both sides of the DC bus. The isolation mechanism, damping and reactive power support functions of the MGP system on grid faults are analyzed by means of the rotor motion equation and phasor diagram of synchronous machine. A 5-kW MGP simulation and experimental platforms are built to verify the isolation and protection effects of the MGP system on a renewable energy generation system during the transient processes of grid voltage sag, overvoltage and multiple voltage sags. The results demonstrate that the MGP system can isolate grid faults on the generator side, while the oscillation amplitude on the motor side is much smaller, and the generator can provide strong reactive power support to the grid during three grid faults.

INDEX TERMS Fault ride-through, high proportion renewable energy grid, motor-generator pair (MGP), multiple voltage sags, fault isolation.

I. INTRODUCTION

With the increasing depletion of fossil fuels and environmental problems, the development of renewable energy generation to replace traditional thermal power plants has become an effective solution. Renewable energy is regarded as the inevitable trend of future electric power development worldwide. With the cost reduction in renewable energy generation and the rapid development of power electronics technology, the proportion of renewable energy generation in the power grid has boomed [1].

However, large-scale disconnection accidents of renewable energy plants caused by grid faults in the power grid have occurred frequently in recent years, which has been a severe challenges for the voltage stability of power grid. These stability issue occur because power electronic converters do not have fault ride-through (FRT) abilities due to the limitations of power electronic devices to withstand voltage and current [2], [3]. Therefore, many countries have issued renewable energy grid connection guidelines, stipulating that renewable energy plants must have required FRT capabilities to improve grid stability [4], [5]. There are two main ways to improve the FRT capabilities of renewable energy units: improving the control strategy of the converter and the auxiliary hardware circuit method. The improved control strategies include de-excitation control [5], virtual impedance control [6], [7], virtual flux control [8]. However, the control effects of the above methods are influenced by

The associate editor coordinating the review of this manuscript and approving it for publication was Lin Zhang.

the severity of the fault and the configuration of the control parameters. The auxiliary hardware circuit methods includes energy storage system [9], rotor crowbar circuits and DC chopper circuit [10], STATCOM, SVC, DVR, and other FACTS devices [11], [12], and stator series impedance [13]. Although these devices can achieve FRT in renewable energy units, there are still many cases of secondary failure due to unreasonable switching during faults. In addition, the number of massive electrical failures caused by extreme weather around the world is increasing each. One typical case is the 9.28 blackout in South Australia [14]. In this event, six transmission line faults occurred due to extreme weather. The first five faults did not induce large-scale wind farm disconnection. The sixth fault caused a 505 MW wind turbine disconnection, resulting in a blackout lasting 50 hours. This incident occurred because renewable energy plants does not have the capability to realize successive FRTs over a very short time, and no effective solution has been reported yet.

The inherent defects in the converter have not been resolved by using the above methods during grid faults. A novel method of grid-connected renewable energy called the motor-generator pair (MGP) was proposed in [15]. Two synchronous machines in the MGP system are coaxially connected, and the renewable energy converters are connected to the synchronous motor while the synchronous generator is connected to the grid. One of the advantages of the MGP system is the isolation function of grid faults on the generator side due to the damping effect of the synchronous machine and the isolation of the mechanical shafting in the MGP system. During the fault, the power output of the renewable energy can be maintained steadily while the excitation of the synchronous generator can be adjusted to support the grid voltage. All these functions can improve the transient stability of the renewable energy power grid.

In this paper, the structure and mathematical model of MGP system are given. The voltage feedback control method of the MGP system is introduced and the isolation, damping and protection mechanism of the MGP system for renewable energy is analyzed. On this basis, the isolation effects of MGP are verified and analyzed by simulation and experiment.

II. STRUCTURE AND MATHEMATICAL MODEL OF MGP SYSTEM

Different from traditional grid connection, renewable energy units can be connected to the grid through the MGP system. As shown in Fig. 1, the MGP system consists of two synchronous machines coaxially connected, and each machine is equipped with an independent excitation system. The capacity of the MGP system matches that of the connected renewable energy units.

The per-unit model is often used to describe the machine. The selections of the stator and rotor reference values for synchronous machines are as follows: the base of stator voltage u_{sb} is the magnitude of the rated stator phase voltage; the base of the stator current i_{sb} is the magnitude of the rated stator phase current; the base of the angular velocity ω_b is the rated

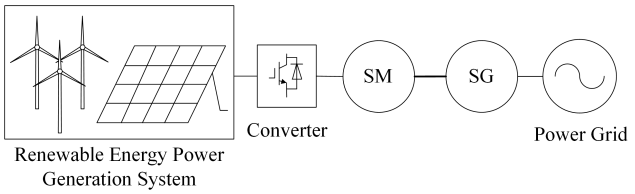

FIGURE 1. Grid-connection through MGP.

stator angular velocity. For the synchronous machine, x_{ad} (the d-axis armature reactance of the synchronous machine) is selected as the rotor base value. Because the two coaxially connected synchronous machines of MGP have the same capacity, the mathematical models of two machines are the same without considering their operation modes of the machines. Therefore, only one machine is used as an example for analysis when modeling the MGP system. With the synchronous motor as an example, the per-unit voltage, current, and motion equations in the d- and q-axis system are given as equations (1)-(3).

$$\begin{bmatrix} U_{sd} \\ U_{sq} \\ U_f \\ U_{Dd} \\ U_{Dq} \end{bmatrix} = R \begin{bmatrix} i_d \\ i_q \\ i_f \\ i_{Dd} \\ i_{Dq} \end{bmatrix} + p \begin{bmatrix} \psi_d \\ \psi_q \\ \psi_f \\ \psi_{Dd} \\ \psi_{Dq} \end{bmatrix} + \begin{bmatrix} -\omega\psi_d \\ \omega\psi_q \\ 0 \\ 0 \\ 0 \end{bmatrix} \tag{1}$$

$$\begin{bmatrix} \psi_{sd} \\ \psi_{sq} \\ \psi_f \\ \psi_{Dd} \\ \psi_{Dq} \end{bmatrix} = \begin{bmatrix} L_d & 0 & L_{ad} & L_{ad} & 0 \\ 0 & L_q & 0 & 0 & L_{aq} \\ L_{ad} & 0 & L_f & L_{ad} & 0 \\ L_{ad} & 0 & L_{ad} & L_{Dd} & 0 \\ 0 & L_{aq} & 0 & 0 & L_{Dq} \end{bmatrix} \begin{bmatrix} i_d \\ i_q \\ i_f \\ i_{Dd} \\ i_{Dq} \end{bmatrix} \tag{2}$$

$$2H \frac{d\omega_m}{dt} = T_e - T_m - K_D \Delta\omega_m \tag{3}$$

where:

R is diag(R_s, R_s, R_f, R_{Dd}, R_{Dq});

R_s, R_s, R_f, R_{Dd}, R_{Dq} are the resistances of the stator winding, field winding, d-axis damper winding, and q-axis damper winding, respectively;

$L_d = L_{ad} + L_{sl}$ and $L_q = L_{aq} + L_{sl}$ are the d- and q-axis synchronous inductances, respectively;

$L_f = L_{ad} + L_{fl}$ is the inductance of the field winding;

$L_{Dd} = L_{ad} + L_{Ddl}$ and $L_{Dq} = L_{aq} + L_{Dql}$ are the inductances of the d- and q-axis damper winding, respectively;

L_{ad} and L_{aq} are the inductances of the d- and q-axis armature reaction inductances, respectively;

L_{sl}, L_{fl}, L_{Ddl} and L_{Dql} are the leakage inductances of the stator winding, field winding, d-axis damper winding, and q-axis damper winding, respectively;

ω, ω_m, ω_{mN}, and $\Delta\omega_m$ are the angular velocity, mechanical angular velocity, rated mechanical angular velocity, and the difference between the electric angular velocity and mechanical angular velocity, respectively;

H is the inertia;

K_D is the damping coefficient;

δ_M is the power angle; and

T_e and T_m are the electromagnetic torque and the mechanical torque, respectively.

Because two synchronous machines are coaxially connected, the MGP system is assumed to be a single mass block model. The speed and variation of the two machines are the same when the MGP system runs steadily. In addition, the mechanical torques sent to the shaft are approximately equal. Therefore, it can be assumed that the two machines have their own electromagnetic equation and share the same motion equation, given as equation (4):

$$2(H_M + H_G)\frac{d\omega_m}{dt} = T_{eM} - T_{eG} - (K_{DG} + K_{DM})\Delta\omega_m \quad (4)$$

where:

H_M, H_G are the inertials of the motor and the generator, respectively;

T_{eM} and T_{eG} are the electromagnetic torques of the motor and generator, respectively; and

K_{DM} and K_{DG} are the damping coefficients of the motor and the generator, respectively.

III. CONTROL METHOD AND ISOLATION PROTECTION MECHANISM OF MGP SYSTEM

A. GRID-CONNECTION CONTROL METHOD OF MGP SYSTEM

The voltage phase difference between the two terminals of the MGP system is proportional to the active power P transferred through the MGP system [16], so P increases with the increase of the phase difference. The above characteristic of the MGP system is the physical basis to realize its stable operation control. Therefore, a DC voltage feedback control method is proposed to achieve active power transmission of renewable energy through the MGP system. The input of the control system is the renewable energy state (wind speed, pitch angle, illumination intensity, ambient temperature, etc.) and the DC link capacitor voltage. The reference DC voltage U_{ref} is calculated based on the maximum power point tracking (MPPT) and the renewable energy state. Then, the reference frequency f_{ref} is calculated by the PI controller from the difference-between U_{dc} and U_{ref}, as shown in Fig. 2.

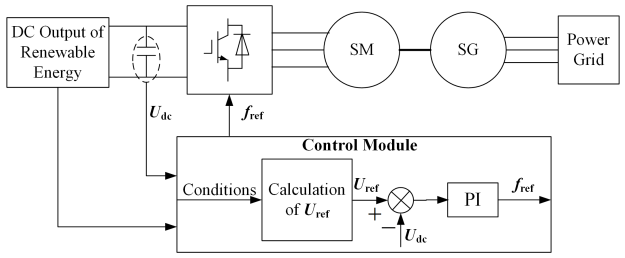

FIGURE 2. DC link voltage feedback control.

The control process is as follows: when $U_{dc} > U_{ref}$, f_{ref} increases. The increase of f_{ref} results in the increase in the frequency of the motor voltage U_M whereas the frequency of the back electromotive force of the two machines and the generator voltage U_G remains unchanged. Therefore, the source-grid difference increases, and P increases accordingly [16]. At the same time, the increase of P leads to an increase in the discharging speed of the DC capacitor, and U_{dc} decreases accordingly. U_{dc} approaches U_{ref} gradually under the feedback control and vice versa.

B. ISOLATION AND PROTECTION MECHANISM OF MGP SYSTEM FOR RENEWABLE ENERGY

Different from traditional FRT methods, the grid voltage fault attacks the synchronous generator firstly. When faults occur on the grid side, the stator and rotor windings of the synchronous generator undergo an electromagnetic transient process and induce transient overcurrent. Compared with the grid-connected converter of renewable energy, synchronous generator has a higher insulation level and overcurrent capacity, and can withstand several times the rated current. In addition, the stator and rotor winding impedances of the machines and the damping effect of the excitation system restrain the magnitude of the overcurrent, and cause the overcurrent to decay rapidly.

Because of the short transient time of voltage fault, it can be assumed that the input power of renewable energy is approximately unchanged. The voltage fault on the grid side leads to an imbalance in the electromagnetic torque at both ends of the shaft. Equation (4) can be transformed into:

$$\frac{d\omega_m}{dt} = \frac{1}{2(H_M + H_G)}\left[T_{eM} - T_{eG} - (K_{DG} + K_{DM})\,\Delta\omega_m\right] \quad (5)$$

The variation of the rotor angular velocity depends not only on the unbalanced torque but also on the inertia and the damping coefficient, as in (5). The MGP system consists of two excitation systems, so the damping coefficient is the superposition of both systems. Moreover, the inertia time constant of the mechanical system of the synchronous machine usually reaches the second level. Therefore, the fluctuation transmitted through the shaft to the motor is obviously decreased, which causes smaller fluctuations in the motor and on the renewable energy side. According to the above analysis, disturbances caused by grid faults are weakened greatly by the shaft of the MGP system which plays an important role in protecting the renewable energy units. Moreover, the damping effect of the MGP system restrains the fluctuations on both sides.

As discussed above, grid faults are isolated and weakened by the MGP system. For the impacts of renewable energy, since the transient process of grid faults is very short, it can be assumed that the wind speed or strength of illumination remains approximately constant. Therefore, the disturbance in renewable energy can be ignored.

In addition, the function of reactive power regulation can not be ignored. The phasor diagram of synchronous generator voltage and current is shown in Fig. 3. When a low-voltage fault occurs in the power grid, the magnitude of the generator terminal voltage $\boldsymbol{U}_L$ is smaller than that of the rated voltage $\boldsymbol{U}_N$. The phasor of the stator current $\boldsymbol{I}_L$ lags that

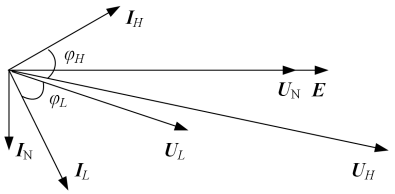

FIGURE 3. Voltage and current phasor diagrams of synchronous generator.

of U_L, and the generator outputs inductive reactive power to the power grid; when an overvoltage fault occurs in the power grid, $U_H > U_N$, I_H is ahead of U_H, and the generator absorbs the excess inductive reactive power in the grid. The above reactive power regulations of the generator are conducive to the rapid recovery of the grid voltage, and can reduce the adverse impact of faults on renewable energy plants.

IV. SIMULATION ANALYSIS OF ISOLATION AND PROTECTION FUNCTIONS OF MGP SYSTEM

In order to verify the isolation and protection function of the MGP system for a renewable energy generation system, a time-domain simulation model is built, as shown in Fig. 4.

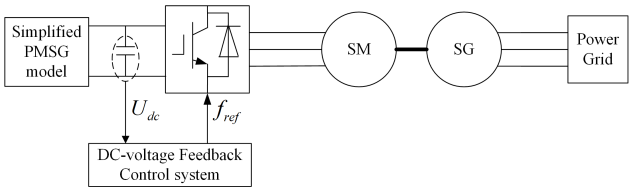

FIGURE 4. Block of simulation model.

A simplified model of magnet synchronous generator (PMSG) is used as simulate a permanent direct-driven wind turbine generator (DWTG), and two synchronous machines with fixed excitation system are coaxially connected to simulate the MGP system. Some of the parameters of the simulation model are shown in Table 1 and Table 2, which are calculated and adjusted based on real 5kW synchronous machine parameters and experiment running data to make the simulation results more reliable.

TABLE 1. Simulation parameters.

Parameters	Value
Nominal line voltage of the AC system /V	380
Renewable energy maximum power /kW	5
Capacity of generator /kVA	5
Capacity of motor /kVA	5
Frequency/Hz	50

The output of the MGP system is approximately 3 kW before the faults. Three kinds of grid faults are set in the power grid module according to the China National Standard [4] and the 9.28 blackout in South Australia [14]. The phase voltage and phase current of two machines, DC link voltage, and frequency of the MGP system are monitored, and then the single-phase power of two machines were calculated respectively. The detailed analyses are as follows:

TABLE 2. Some of the motor parameters in the simulation model.

Parameters	Value	Parameters	Value
R_s	0.03	L_{sl}	0.0008
R_f	0.001	L_{fl}	0.0003
L_d	2.04	L_{Ddl}	0.000005
L_q	1.93	L_{Dql}	0.0002

A. VOLTAGE SAG CONDITION

A decrease in the grid voltage from 220 V to 44 V (0.2p.u.) is set at 15 s and the recovery to 220 V is set at 20 s. The results are shown in Fig. 5.

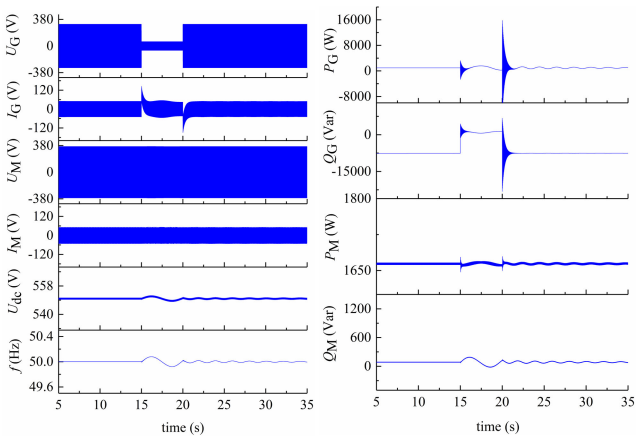

(a) (b)

FIGURE 5. LVRT simulation results for MGP system. (a) voltage, current, and frequency; (b) active power and reactive power.

As shown in Fig. 5, the generator current increases instantaneously when voltage sag occur, which leads to the torque imbalance in the shafting. The power of the synchronous generator oscillates and decays under the damping effect. Due to the isolation of the shafting, the power oscillation amplitude of the synchronous motor is much smaller than that of the synchronous generator. The DC link voltage and frequency oscillate and attenuate due to unbalanced power on both sides of the capacitor. However, the voltage oscillation amplitude of capacitor is no larger than 0.37% of the reference DC voltage because of the function of the control system. From Fig. 5 (b), it can be seen that the active power output by the generator to the power grid fluctuate, but the voltage and current of the motor stay almost unchanged compared to those of the generator. A major part of the increasing current is the reactive current generated by the voltage difference, which can provide inductive reactive power support to the grid.

During voltage recovery, the active power output of the MGP system can gradually recover to its original state after a transient process. The DC link voltage fluctuates within a small range during the voltage sag, demonstrating that the DWTG is less influenced by the grid voltage sag.

B. OVERVOLTAGE CONDITION

The voltage RMS value on the grid side is set to swell from 220 V to 286 (1.3 p.u.) at 15 s and recover to 220 V at 20 s. The results are shown in Fig. 6.

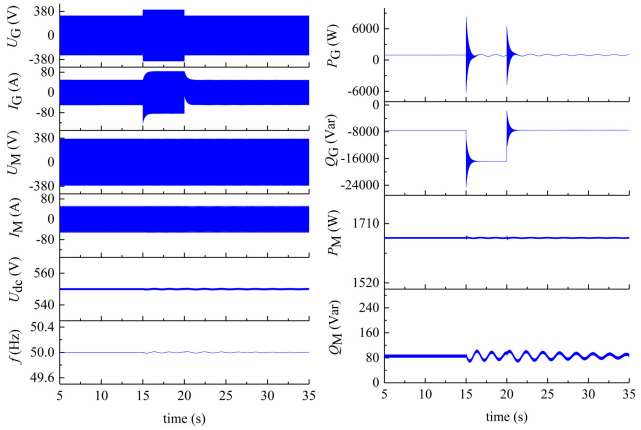

FIGURE 6. HVRT simulation results for MGP system. (a) voltage, current, and frequency; (b) active power and reactive power.

As shown in Fig. 6, when the grid voltage swells to 1.3 p.u., the generator withstands the impact of overvoltage and overcurrent while the oscillation on the motor side can be neglected with the help of DC voltage feedback control. Compared with the results in section A, the voltage oscillation amplitude of the capacitor is much smaller because the voltage change amplitude of the grid is only 3/8 of the voltage sag. The key to the HVRT of renewable energy through the MGP system is a reliable insulation level in the generator. Due to the sudden increase of grid voltage, the excitation current of synchronous generators can not provide enough air gap magnetic field. The voltage difference causes the generator to absorb reactive power, promoting grid voltage recovery. Although the change in the speed leads to small fluctuations in the voltage and current of the motor, the DWTG can maintain stable operation under the adjustment of the control system. After a dynamic process (similar to the low voltage process), the active power output of the MGP system can also gradually return to its original state.

C. MULTIPLE VOLTAGE SAGS CONDITION

Referring to the blackout in South Australia, multiple voltage sags are set at 22.7 s, 48.7 s, 75 s, 96.7 s, 102.7 s, and 106.7 s respectively. The phase voltage of the power grid sags from 220 V to 176 V, 132 V, 132 V, 88 V, 88 V, and 88 V successively. Each voltage drop lasts one second and then the voltage recovers to 220 V, as shown in Fig. 7.

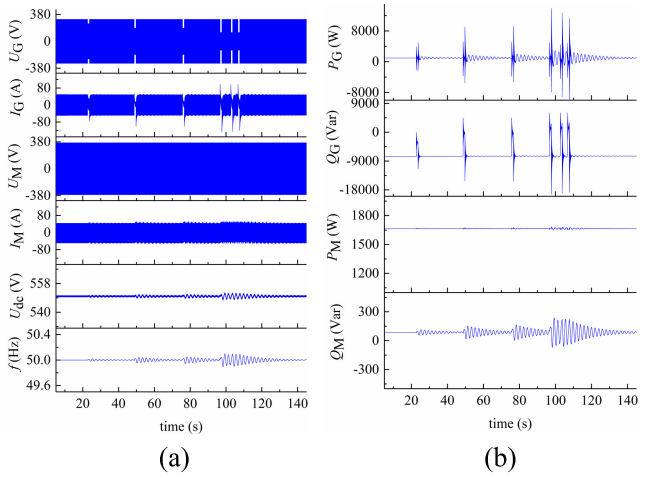

FIGURE 7. LVRT simulation results for MGP system. (a) voltage, current, and frequency; (b) active power and reactive power.

As shown in Fig. 7, the magnitudes of the generator current increase with the increasing severity of the grid voltage sag. Because of the short intervals between the last three voltage sags, the transient process caused by the fault is superimposed, resulting in large fluctuations in the power output by the generator, which is reflected in the increasing voltage oscillations of the capacitor. However, the motor current and DC link voltage fluctuate slightly because of the isolation and damping functions of the MGP system. Fig. 7 (b) shows that the active power output of MGP system is basically stable with the large fluctuations of the first several cycles. Because of the torque imbalance, there are also fluctuations in the motor voltage and current, but these fluctuations are very small, and the output of DWTG can gradually return to the previous level after the voltage recovery. Overall, the operation of the MGP system can be stable during the six voltage sags.

V. EXPERIMENTAL VERIFICATION OF MGP ISOLATION AND PROTECTION RENEWABLE ENERGY SYSTEM

An experimental bench is built in the laboratory to simulate the connection of the DWTG unit to the grid through the MGP system, as shown in Fig. 8.

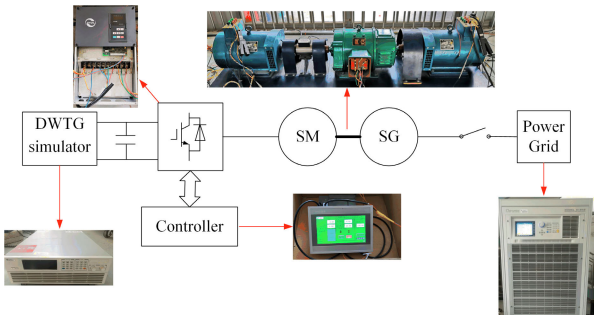

FIGURE 8. MGP grid-connection experimental bench for DWTG unit.

The bench includes a 10 kW DWTG emulator, a 30 kW converter, an MGP system (including two coaxially

TABLE 3. Parameters of synchronous machine.

Parameters	Value	Parameters	Value
R_s	0.003	L_{sl}	0.13
R_f	0.0006	L_{fl}	0.076
L_d	2.04	L_{Ddl}	0.229
L_q	1.93	L_{Dql}	0.0812

connected STC-5 synchronous machines), and a Chroma 61845 power grid simulator. The parameters of the synchronous machines are shown in Table 3, and other parameters are consistent with Table 1. The DWTG emulator is used to emulate the DC output power characteristics of the rectifier connected to the PMSG. The function of the grid emulator is to emulate the grid and set the grid voltage fault.

To verify the isolation and protection functions of the MGP system for renewable energy units, three kinds of grid faults are set with the power grid emulator according to the China National Standard and the 9.28 blackout in South Australia. The phase voltage and phase current of two machines, DC-bus voltage, and frequency of the MGP system are measured by a Yokogawa scope corder, and then the output power of the MGP system is calculated. At the beginning of the experiment, the DC voltage of the converter is 580 V and the output active power of MGP system is approximately 1.3kW under both low-voltage and overvoltage fault. The specific experimental process and results are as follows:

A. LOW-VOLTAGE FAULT

With the grid emulator, a decrease in the voltage from 220 V to 44 V is set at 18 s, and the recovery to 220 V is set at 23 s. The results are shown in Fig. 9.

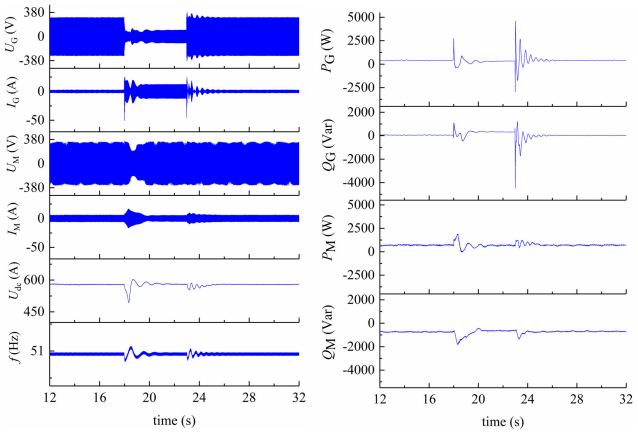

FIGURE 9. LVRT experimental results for MGP system. (a) voltage, current, and frequency; (b) active power and reactive power.

Fig. 9 (a) shows that the peak value of the generator current under the fault is over 10 times that under steady-state operation, accompanied with severe oscillations at the same time. The experimental results are worse than the simulation results because the experimental synchronous machine is different from the synchronous generator of the thermal power plant in terms of the shafting structure, damping effects and quality of windings and iron core. However, the peak value of the motor current under the fault is no more than 2 times that under the steady-state operation. After several cycles, the output active power of the generator is stable and the inductive reactive power output is approximately 1 kVar, as shown in Fig. 9 (b). The fluctuations of voltage and current caused by the torque imbalance of the rotor shafting are relatively small due to the isolation and damping effects of the MGP system, and the output power of the DWTG emulator can be kept stable.

B. OVERVOLTAGE FAULT

A swell of the emulated grid voltage from 220 V to 286 V is set at 19 s, and the emulated grid voltage recovers to 220 V at 24 s. The results are shown in Fig. 10.

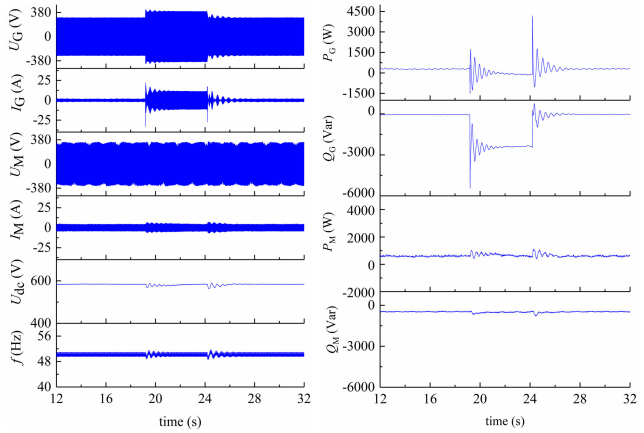

FIGURE 10. HVRT experimental results of MGP system. (a) voltage, current, and frequency; (b) active power and reactive power.

Fig. 10 (a) shows that the stator current of the generator increases instantaneously when the voltage swells. A similar transient process during both the voltage sag and swell is found when comparing Fig. 9 and Fig. 10. The experimental results show the fluctuation in the output power during the low-voltage process is larger than that during the overvoltage process due to the differences in the variation of the voltage magnitude. Overall, the overvoltage tolerance of the generator is the key to the realization of HVRT. As in Fig. 10 (b), the power of the generator tends to be stable after rapid attenuation while the power of the motor fluctuates within a small range. The fluctuations of the voltage and current of the motor, DC link voltage, and frequency are very small. The above analysis shows that the MGP system isolates the grid fault on the generator side and maintain steady operation during grid voltage swell. In addition, the generator absorbs inductive reactive power of approximately 2.5 kVar, which provides strong support to maintaining the voltage stability of the power grid.

C. MULTIPLE LOW-VOLTAGE FAULTS

The DC link voltage is set as 570 V, and the output active power of the MGP system reaches 900 W. Referring to the blackout in South Australia, multiple low-voltage faults are set at 7.7 s, 33.7 s, 60.7 s, 81.7 s, 87.7 s, and 91.7 s. The six sags of the emulated grid voltage are set from 220 V to 176 V, 132 V, 132 V, 88 V, 88 V, and 88 V successively. Each voltage drop lasts one second and then the voltage recovers to 220 V, shown in Fig. 11.

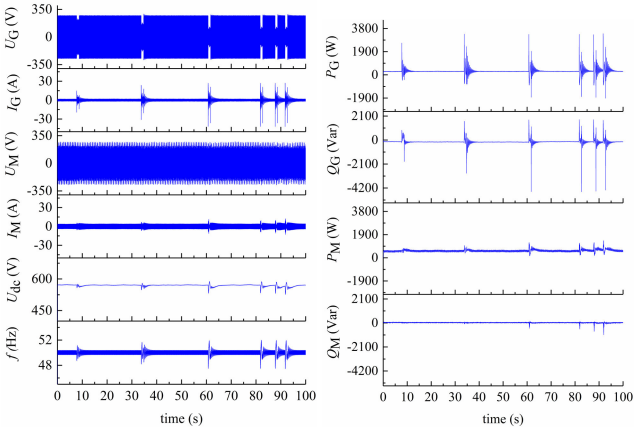

FIGURE 11. Multiple LVRT experimental results for MGP system. (a) voltage, current, and frequency; (b) active power and reactive power.

Fig. 11 shows the fluctuation magnitudes on both the motor and generator side increase with the increasing amplitude of voltage sag during the multiple low-voltage faults. Compared with the low-voltage faults in the South Australia grid, all six low-voltage faults are ridden through by the MGP system while the voltage and current fluctuations of the motor are relatively small. During the last three faults, due to the short time interval between the faults, the transient process of two adjacent faults appears with superposition effect, which leads to larger power fluctuations on both sides of the MGP system. Due to the isolation and protection function of the MGP system, the output power of the DWTG emulator can still maintain a relatively stable power grid through the MGP system. However, the oscillation amplitudes in Fig. 11 are quite large since the mechanical connection and quality of the two synchronous machines are poor. This problem can be solved by referring to the technology of large capacity synchronous generator applied in the thermal power plant.

VI. CONCLUSION

In this paper, the isolation and protection mechanism and reactive power support function of the MGP system are analyzed based on the rotor motion equation and the phasor diagram of voltage and current. The following conclusions are drawn through simulation and experiment:

1) When a grid fault occurs, the MGP system can isolate the fault at the generator side and protect the renewable energy units from disconnection. Because the inertia of the MGP shaft is on the level of second, the voltage and current fluctuations at the motor side caused by the power imbalance are small, and the output power on both sides is relatively stable with the adjustment of the DC voltage feedback control.

2) When the grid voltage sags several times over a short time, the transient process superposes to the next process due to the short fault interval, and the synchronous generator can still withstand the impact of overcurrent caused by each fault. With the isolation and damping effect of the MPG system, the voltage and current of the renewable energy generation system fluctuate slightly.

3) The excitation system of the synchronous generator can provide not only damping but also reactive power support during the grid faults, which is conducive to grid voltage recovery.

REFERENCES

[1] Y. Yang, H. Wang, F. Blaabjerg, and T. Kerekes, "A hybrid power control concept for PV inverters with reduced thermal loading," *IEEE Trans. Power Electron.*, vol. 29, no. 12, pp. 6271–6275, Dec. 2014, doi: 10.1109/tpel.2014.2332754.

[2] S. Alepuz, S. Busquets-Monge, J. Bordonau, J. Martinez-Velasco, C. Silva, J. Pontt, and J. Rodriguez, "Control strategies based on symmetrical components for grid-connected converters under voltage dips," *IEEE Trans. Ind. Electron.*, vol. 56, no. 6, pp. 2162–2173, Jun. 2009, doi: 10.1109/tie.2009.2017102.

[3] M. Mohseni and S. M. Islam, "Review of international grid codes for wind power integration: Diversity, technology and a case for global standard," *Renew. Sustain. Energy Rev.*, vol. 16, no. 6, pp. 3876–3890, Aug. 2012, doi: 10.1016/j.rser.2012.03.039.

[4] *Testing Rules for Fault Voltage Ride-through Capability of Wind Turbine Generators*, China Standard GB/T 36995, 2018.

[5] L. Ran, D. Xiang, P. Tavner, and S. Yang, "Control of a doubly fed induction generator in a wind turbine during grid fault ride-through," in *Proc. IEEE Power Eng. Soc. Gen. Meeting*, Jun. 2006, p. 1, doi: 10.1109/pes.2006.1709162.

[6] Z. Xie, X. Zhang, X. Zhang, S. Yang, and L. Wang, "Improved ride-through control of DFIG during grid voltage swell," *IEEE Trans. Ind. Electron.*, vol. 62, no. 6, pp. 3584–3594, Jun. 2015, doi. 10.1109/TIE.2014.2370938.

[7] S. Hu, X. Lin, Y. Kang, and X. Zou, "An improved low-voltage ride-through control strategy of doubly fed induction generator during grid faults," *IEEE Trans. Power Electron.*, vol. 26, no. 12, pp. 3653–3665, Dec. 2011, doi: 10.1109/tpel.2011.2161776.

[8] R. Zhu, Z. Chen, X. Wu, and F. Deng, "Virtual damping flux-based LVRT control for DFIG-based wind turbine," *IEEE Trans. Energy Convers.*, vol. 30, no. 2, pp. 714–725, Jun. 2015, doi: 10.1109/tec.2014.2385966.

[9] C. Abbey and G. Joos, "Supercapacitor energy storage for wind energy applications," *IEEE Trans. Ind Appl.*, vol. 43, no. 3, pp. 769–776, 2007, doi: 10.1109/tia.2007.895768.

[10] A. M. A. Haidar, K. M. Muttaqi, and M. T. Hagh, "A coordinated control approach for DC link and rotor crowbars to improve fault ride-through of DFIG-based wind turbine," *IEEE Trans. Ind Appl.*, vol. 53, no. 4, pp. 4073–4086, Jul. 2017, doi: 10.1109/tia.2017.2686341.

[11] M. Molinas, J. Are Suul, and T. Undeland, "Low voltage ride through of wind farms with cage generators: STATCOM versus SVC," *IEEE Trans. Power Electron.*, vol. 23, no. 3, pp. 1104–1117, May 2008, doi: 10.1109/tpel.2008.921169.

[12] A. O. Ibrahim, T. H. Nguyen, D.-C. Lee, and S.-C. Kim, "A fault ride-through technique of DFIG wind turbine systems using dynamic voltage restorers," *IEEE Trans. Energy Convers.*, vol. 26, no. 3, pp. 871–882, Sep. 2011, doi: 10.1109/tec.2011.2158102.

[13] Y. Xiangwu, G. Venkataramanan, W. Yang, D. Qing, and Z. Bo, "Grid-fault tolerant operation of a DFIG wind turbine generator using a passive resistance network," *IEEE Trans. Energy Convers.*, vol. 26, no. 10, pp. 2896–2905, Oct. 2011, doi: 10.1109/TPEL.2010.2087037.

[14] *Update Report-Black System Event In South Australia*, Austral. Energy Market Operator, Adelaide, Australia, Oct. 2016.

[15] S. Wei, Y. Zhou, S. Li, and Y. Huang, "A possible configuration with motor-generator pair for renewable energy integration," *CSEE J. Power Energy Syst.*, vol. 3, no. 1, pp. 93–100, Mar. 2017, doi: 10.17775/CSEE-JPES.2017.0012.
[16] Y. Zhou, G. Xu, S. Wei, X. Zhang, and Y. Huang, "Experiment study on the control method of motor-generator pair system," *IEEE Access*, vol. 6, pp. 925–936, 2018, doi: 10.1109/access.2017.2776974.

YUJUN GU (Student Member, IEEE) was born in Jilin, China, in 1990. He received the B.E. degree in electrical engineering and automation from Northeast Electric Power University, Jilin, China, in 2013, and the M.E. degree in power system and automation from North China Electric Power University, Beijing, Hebei, China, in 2016, where he is currently pursuing the Ph.D. degree with the School of Electrical and Electronic Engineering.

His research interest mainly includes the stability of power systems with renewable energy.

YONGZHANG HUANG (Member, IEEE) received the B.S. degree from the Department of Engineering Physics, Tsinghua University, Beijing, China, in 1984, and the Ph.D. degree in physics from the Chinese Academy of Sciences, in 1991.

He is currently a Professor with NCEPU. His research interests include renewable energy power systems, high power electronic device and application, electric vehicle, and big data of power grid.

QIANYU WU (Student Member, IEEE) was born in Shanxi, China, in 1994. She received the B.E. degree in electrical engineering and automation and the M.E. degree in power system and automation from North China Electric Power University, Beijing, China, in 2015 and 2018, respectively, where she is currently pursuing the Ph.D. degree with the School of Electrical and Electronic Engineering. Her research interest mainly includes the stability of power systems with renewable energy.

CHENYANG LI (Student Member, IEEE) was born in Henan, China, in 1996. He received the B.E. degree in electrical engineering and automation from North China Electric Power University, Beijing, Hebei, China, in 2013, where he is currently pursuing the M.E. degree with the School of Electrical and Electronic Engineering. His research interest mainly includes the stability of power systems with renewable energy and power electronics.

HAISEN ZHAO (Member, IEEE) was born in Hebei, China, in 1982. He received the B.E. degree in agricultural electrification and automation from the Agriculture of Hebei, Baoding, China, in 2004, and the M.E. and Ph.D. degrees in electric machines and apparatus from North China Electric Power University, Beijing, China, in 2007 and 2011, respectively.

He is currently an Associate Professor with NCEPU. His research interests include electrical machines design, operation performance, energy consumption analysis on electrical machines, and motor system energy saving.

YANG ZHAN (Member, IEEE) was born in Beijing, China, in 1978. He received the B.E. and M.E. degrees in electric engineering from Tsinghua University, Beijing, China, in 2001 and 2004, respectively, and the Ph.D. degree in power engineering and power electronics from the University of Alberta, Edmonton, Canada, in 2010.

After graduation, he was at Andritz Hydro Ltd., Peterborough, ON, Canada, as an Electromagnetic Analysis Engineer for three years, and Powertech Labs Inc., Surrey, BC, Canada, as a Power System Software Development Engineer for almost two years. He is currently an Associate Professor with North China Electric Power University, Beijing. His research interests include numerical modeling, loss analysis, and design optimization of electrical machines.